NASA CR-144694

15 OCTOBER 1975

EXPERIMENT DEFINITION PHASE SHUTTLE LABORATORY

LDRL-10.6 EXPERIMENT

•

Fifth Quarterly Report

NASA Contract NAS 5-20018

(NASA-CR-144694) EXPERIMENT DEFINITION PHASE SHUTTLE LABORATORY LDRL-10.6 EXPERIMENT Quarterly Report, 27 Jun. - 26 Sep. 1975 (Hughes Aircraft Co.) 28 p HC $4.00 CSCL 22C G3/12

N76-13129

Unclas

05686

HUGHES

HUGHES AIRCRAFT COMPANY
SPACE AND COMMUNICATIONS GROUP

Hughes Ref. No. D0824 • SCG 50322R

CONTENTS

1. INTRODUCTION

This fifth quarterly report for the Experiment Definition Phase of the Shuttle Laboratory LDRL 10.6 Micrometer Experiment (Contract NAS 5-20018) covers period 27 June through 26 September 1975. Activities during the fifth quarter included:

- Reevaluation of system obscuration ratio with a subsequent reduction of this ratio from 0.417 to 0.362
- Completion of detail drawings for the 6X pre-expander; negotiations with vendor completed and item ordered
- Completion of detail drawings for the nine mirrors that comprise pointing and tracking optomechanical subsystem (OMSS); extensive modifications to drawings required during negotiations with vendor; modifications complete and mirrors ordered
- Continuation of detailing of mechanical portions of OMSS; modifications to accommodate new obscuration ratio completed; details more than 95 percent complete
- Qualitative operation of the optomechanical subsystem of the 10.6 μm receiver achieved under experiment measurement task; receiver fully integrated and operation demonstrated over a 10 km experimental link
- Data collection task initiated to begin preparation of link analysis volumes

2. SCHEDULE

Several potential problem areas were eliminated during this quarter, including: a change in the obscuration ratio which required a revision of many of the completed drawings; redesign and negotiations with vendors which became necessary when bids on beryllium parts came in with a 54 percent price increase over original estimates; and finally, delays caused by these problems caused conflicts between schedules on other programs, with the result that several people were unable to work when needed.

All of these problems have been resolved but at a cost in time. Accordingly, a revised schedule has been generated as shown in Figure 1. The primary change was a reduction in the fabrication time, requiring parallel manufacture of the various subsystems. This has been coordinated with shop and vendors and will not cause any problems. There was sufficient slack built into the original schedule to allow for the present slippage; the system will still be completed by 1 March 1976.

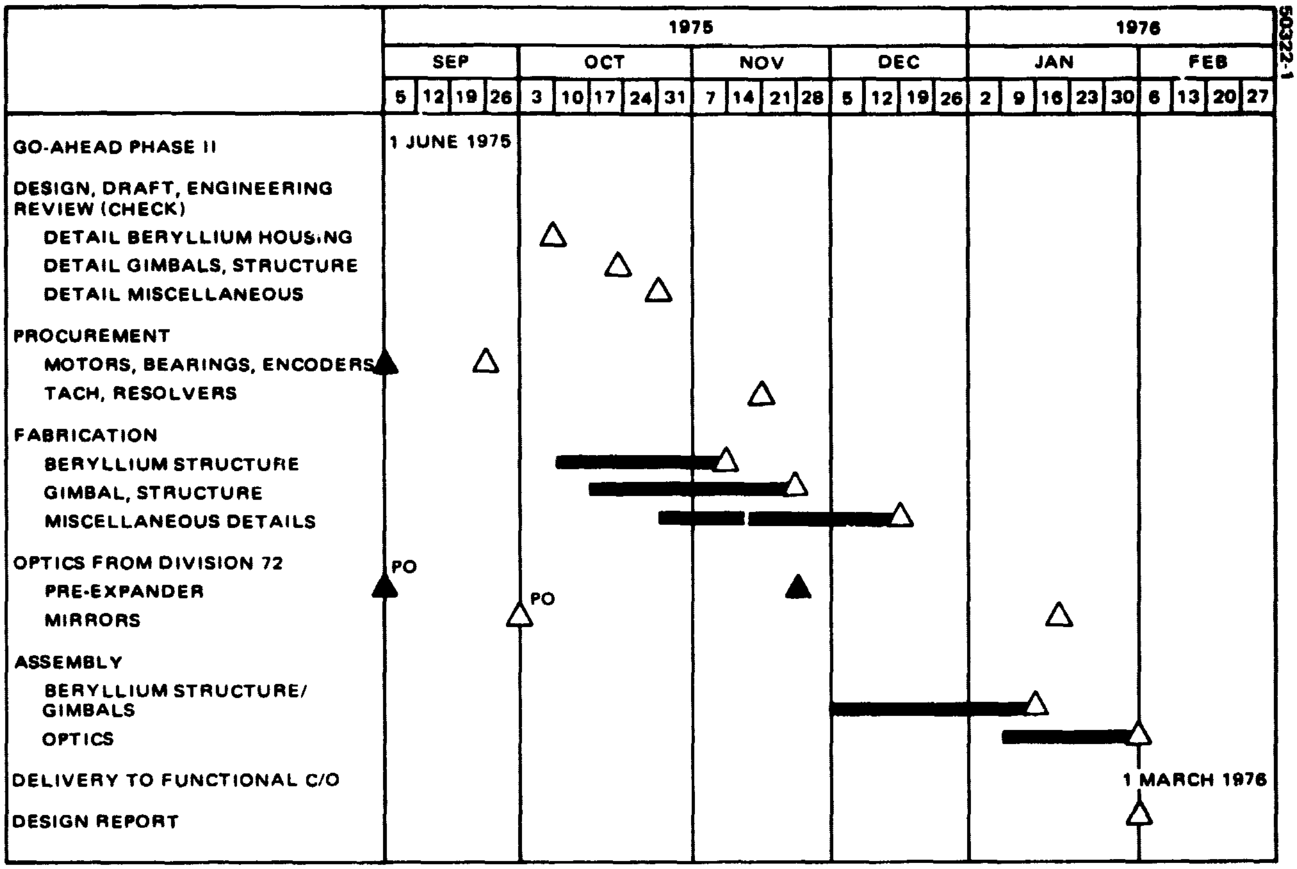

FIGURE 1. REVISED SCHEDULE FOR LDRL 10.6 MICROMETER ENGINEERING MODEL

3. OBSCURATION RATIO

The effective obscuration ratio for the LDRL telescope is a critical parameter that must be minimized, since this obscuration occurs at the highest energy density region of the Gaussian illumination function. Consequently, the parameter was reexamined to determine the source of the 0.417 ratio. Obscuration occurs because there must be a hole in the image plane folding mirror of sufficient size to accommodate the required field of view as shown in Figure 2. The investigation revealed that there are two obscurations involved; the physical obscuration caused by the hole itself, and an additional effective obscuration caused by the imperfections in the mirror surface near the edge of the hole.

Assuming that no vignetting is to be allowed over the entire 1° field of view, the minimum obscuration ratio was originally determined to be 0.299. In the original plan, an alignment tolerance of ±0.5 mm was added to the hole size, corresponding to a physical obscuration ratio of 0.338. A 1 mm chamfer around the edge of the hole in the mirror caused an additional obscuration that corresponds to the specified 0.417.

Unfortunately, the 0.417 ratio was interpreted by the mechanical designers as the physical obscuration ratio, and mirrors were designed with a hole that corresponds to this ratio. Had the mirrors been fabricated, the total obscuration would have been 0.496, allowing for the 1 mm chamfer.

The source of the 0.299 obscuration ratio was a graphical analysis of the region near the primary focal plane. During the reevaluation a more exact technique was used for determining this ratio. In Figure 2, the limit ray is labeled. Figure 3 shows the geometric analysis performed

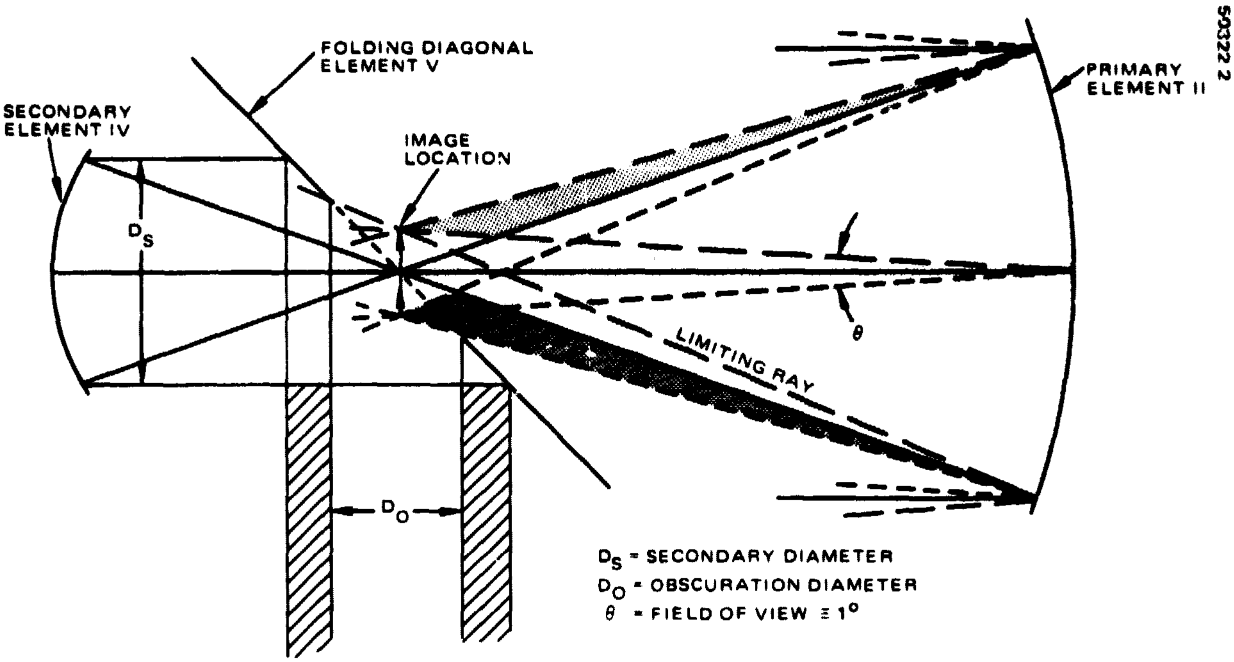

FIGURE 2. ORIGIN OF OBSCURATION FOR FINITE FIELD OF VIEW GREGORIAN CONFIGURATION

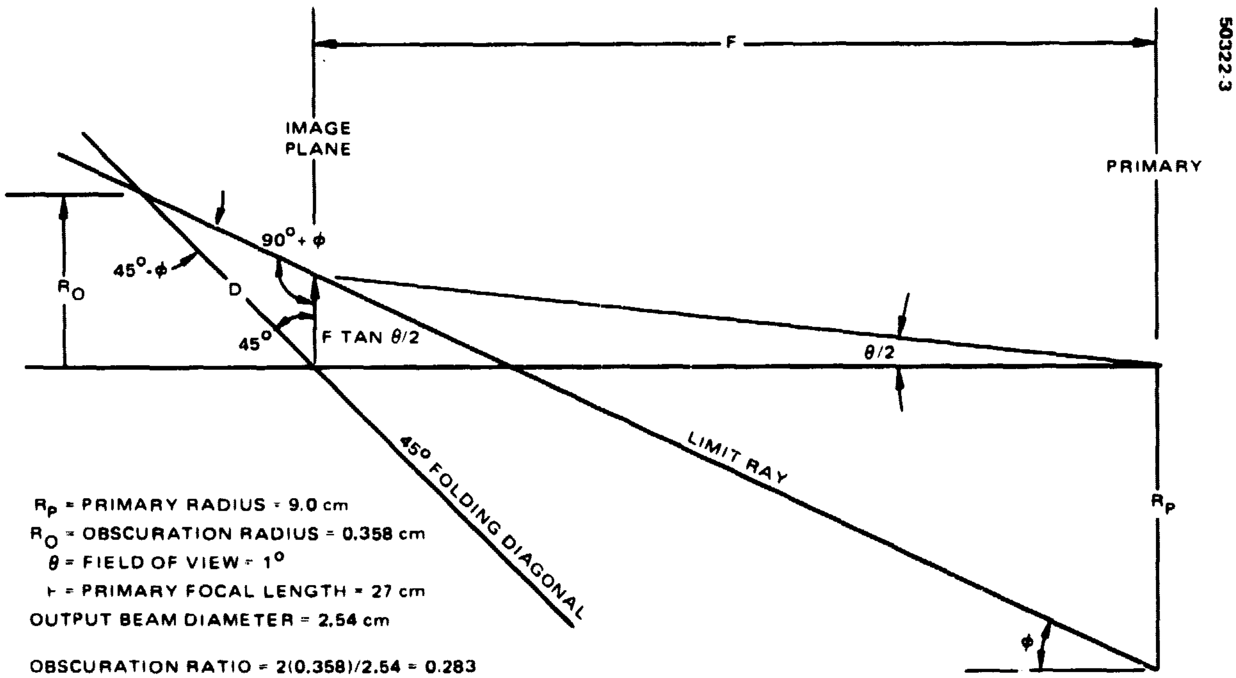

FIGURE 3. GEOMETRIC DETERMINATION OF MINIMUM OBSCURATION RATIO

to determine the obscuration ratio necessary to accommodate this ray. From this analysis the minimum obscuration ratio for a 1° clear field of view is 0.283.

The ±0.5 mm alignment tolerance was incorporated to assure that a clear 1° field of view centered on the optic axis would be available. During reevaluation, it was decided that this tolerance was unnecessary since, regardless of location of the hole, a 1° clear field of view will exist. Thus, the physical obscuration caused by the hole in element 5 will be 0.283. The total obscuration, allowing for a 1 mm edge chamfer, will be 0.362. This number is being used as the ratio for all link power budget calculations. The 1 mm chamfer is conservative; an effort will be made during manufacture to maintain mirror figure closer than 1 mm from the edge to improve performance.

The program has been impacted in several areas. First, the mirror drawings had to be modified to incorporate the new hole sizes in both element 2 (large folding mirror) and element 5 (small folding mirror that determines the obscuration ratio). Secondly, the reduction of hole size in element 2 requires that this element be shifted towards the secondary mirror by approximately 1 inch in order to prevent vignetting of outer rays from the primary mirror. This change will require several drawings to be changed or replaced. To minimize this impact, element 2 was not moved but elements 3, 4, and 5 were moved relative to element 2. Thirdly, shifting of the various components has reduced space available for the IMCs. The reduced space will not interfere with the GTE IMCs, but might interfere with one of the contemplated magnetic designs. However, if this should prove to be the case, most of the lost space can be recovered by notching the back of element 2.

Figure 4 shows the space available for IMC 2. Originally, the space allocated was 1.5 by 2 by 3 inches for each IMC as discussed in the third quarterly report. Figure 5, reproduced from the same third quarterly report, shows the two concepts considered for the IMC and also the basis for the chosen dimensions. The loss of one corner of space allocation

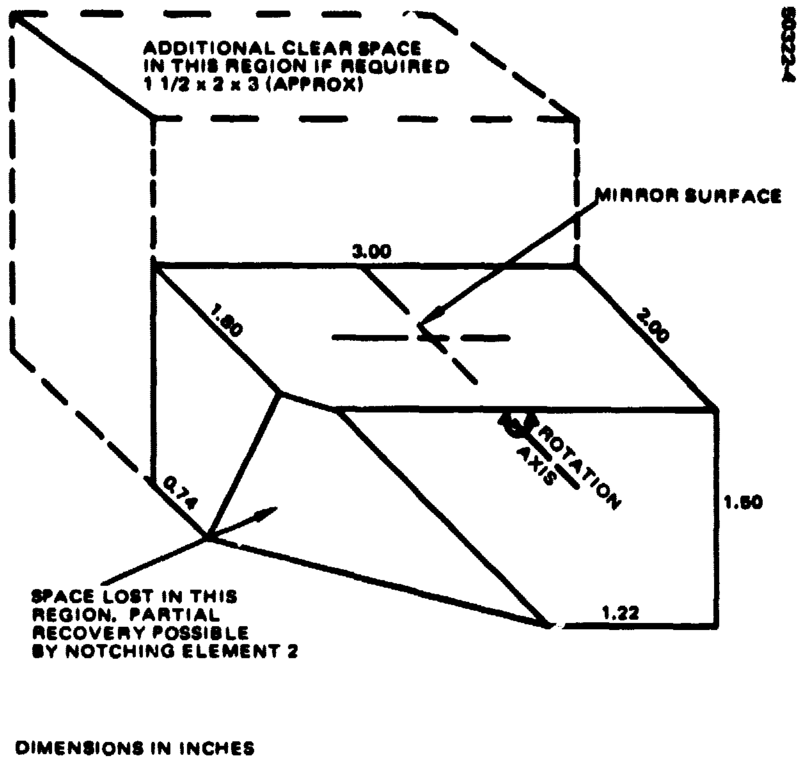

FIGURE 4. SPACE ALLOCATION FOR IMC 2

might compromise the field coil approach, requiring the notching of element 2 to regain part of this loss. For the motor driven concept, no change would be required. Finally, there is additional clearance in the OMSS to allow extension of the 3 inch dimension, thus providing additional clearance in the area where the motor would be located.

In summary, the modifications necessary to accommodate the change in obscuration ratio are relatively minor. The primary benefit of this change is nearly a 50 percent increase in transmitted power (1.35 dB). It is clear that the performance increase is well worth the modification.

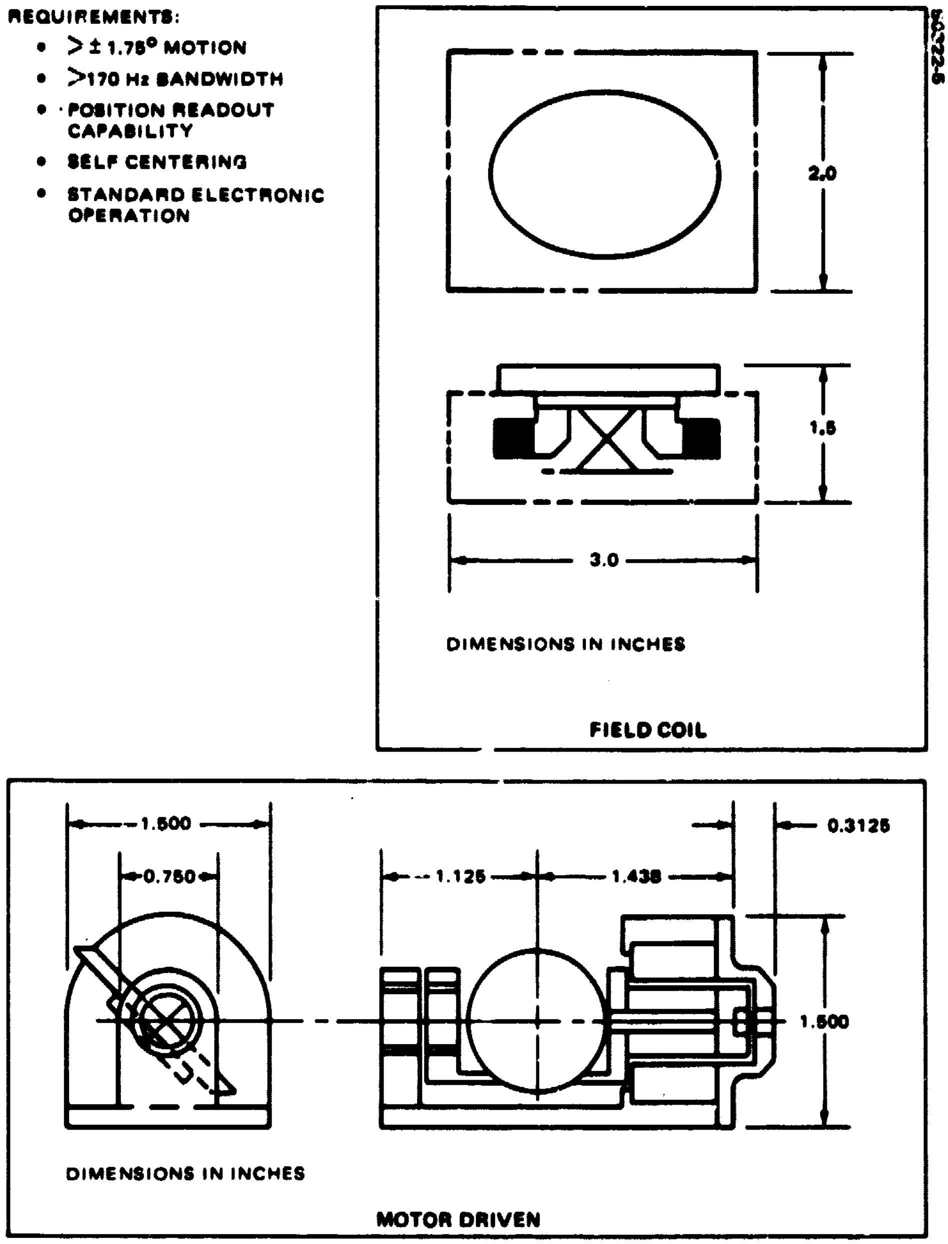

FIGURE 5. IMC CONCEPTS

4. OPTICS

PRE-EXPANDER

During this quarter all pre-expander drawings were completed and submitted to five vendors for competitive bids. The five vendors are:

1) A ied Optics Center (AOC)

2) Space Optics Research Labs (SORL)

3) Perkin Elmer

4) Tinsley Laboratories

5) Fecker Systems

Tinsley and Fecker are experiencing a heavy work load and declined to bid. Bids from the other three vendors were technically acceptable with only minor exceptions to the offered specifications, primarily in mechanical tolerances. None of the exceptions would materially degrade performance. Delivery from all vendors was 12 weeks ARO.

The only significant difference between bidders was price, with a spread of approximately 50 percent. SORL was selected, primarily because they submitted the lowest bid, but also because of the degree of cooperation during negotiations and their obvious interest in this task. The order was placed 25 August and delivery is presently scheduled for 17 November 1975.

Figure 6 is the assembly drawing for the pre-expander telescope.

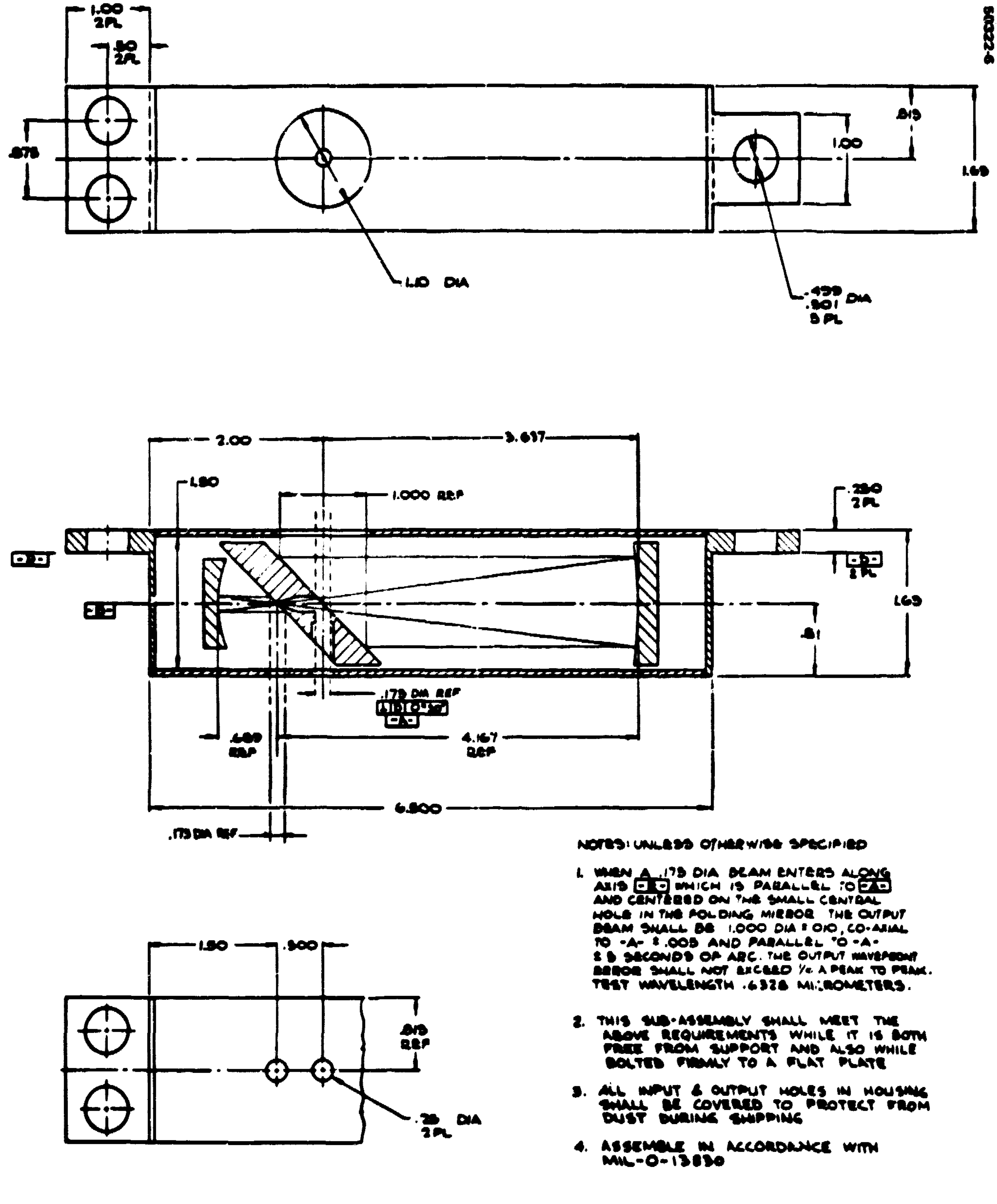

FIGURE 6. PRE-EXPANDER ASSEMBLY DRAWING (3482109)

Nine Mirrors for OMSS

The nine mirrors comprising the large beam expander were originally planned to be fabricated from beryllium. The pricing for these items was based on a rough order of magnitude (ROM) bid received from Applied Optics Center during the proposal effort for this contract. A set of engineering drawings was prepared and sent to five potential vendors during July. The following responses to the RFQ were received for the beryllium mirrors on approximately 20 August 1975:

1) Schiller Industries ($32,000)

2) Applied Optics Center ($26,000)

3) Perkin Elmer (no bid)

4) Tinsley (no bid)

5) Contravis-Goerz (no response)

The lowest bid reflected an increase of 54 percent over the earlier ROM bid (15 January 1975) of $17,000. The increase was principally due to an increased cost of beryllium material and mirror machining. Because of a desire to design the brassboard in as near a flight configuration as is practical, a compromise was agreed to on the design of the mirrors, elements 1 through 9. Elements 1, 6, 7, 8, and 9 were changed to 6061-T6 aluminum and elements 2, 3, 4, and 5 were changed from composition D to HMS 20-1611 composition A beryllium. Element 3, the primary mirror, was redesigned to include bonding the rear alignment/holding portion to the primary mirror, to reduce the size of beryllium blank required. An additional RFQ reflecting the above redesigns was reissued on 10 September 1975.

Bids were resubmitted in two categories:

1) Material and fabrication of beryllium mirrors: bids by American Beryllium Co. (ABC) and Paramount

2) Total fabrication, polishing, and coating of both aluminum and beryllium mirrors: bids by Applied Optics Center (AOC) and Schiller Industries

All bids were received by 17 September with the lowest bids submitted by ABC and AOC. The AOC bid reflected an 18 percent increase over their original ROM bid.

After arriving at an agreement on changes indicated in Section 3, the mirror orders were placed 19 September to AOC, who will subcontract the beryllium material procurement and beryllium mirror fabrication to ABC. All changes received approval of the contract monitor. Mirrors are scheduled for delivery to Hughes on 15 January 1976.

Tolerance Analysis

The present optical system is very similar to the previously built receiver discussed in Section 7. An extensive analysis was carried out on the receiver to show that this type of optics is insensitive to nearly any alignment tolerance except mirror spacing, and that the materials and structural designs of the system satisfactorily hold the critical focus adjustments. Based on previous experience and because of the increased costs incurred in purchasing the optics, a decision was made to terminate work on the tolerance analysis. Analysis can be carried out at a later date if deemed necessary. This decision was cleared with the contract monitor.

5. MECHANISMS AND STRUCTURE

Principal effort during this quarter was the continuing preparation of detail drawings of various elements of the inner and outer gimbals, as well as the telescope housing box. Detailed drawings include the inner and outer gimbal shaft and housing and supports for the small folding mirror (element 5). Ninety-five percent of the total drawings required are now complete. Table 1 is an updated indentured drawing list.

The stress analysis group completed its review of the beryllium box structure and found it to be satisfactory for potential launch environment. Comments from the beryllium fabrication facility were incorporated into the drawing. Fabrication of steel end plates and some of the mirror mounts has begun. Figure 7 is the updated layout drawing (3 pages) for the optomechanical subsystem.

As a result of an analysis performed on the telescope optics, it was determined that system obscuration ratio would not be 0.417 as originally planned, but would be reduced to 0.362. As a direct result of the changes in the optical elements (smaller hole in element 2), a detailed layout was made to determine the effects on the optomechanical subsystem. The modifications required the lengthening of the optical box to move the primary mirror outboard by 1 inch. Additionally, the secondary small folding mirror and IMCs were also shifted outboard by the same amount. Drawings have been revised accordingly.

Because of the change in mirror material from beryllium to aluminum to decrease costs, and the associated mirror thickness changes (elements 5 through 9), a reexamination of some of the mirror supports was made to ensure optical compatibility.

Some of the long lead time procured elements were received and are being processed into the bonded stores for such hardware. These are the gimbal bearings and instrument cluster drive gears.

TABLE 1. INDENTURED DRAWING LIST

3484001	Transmitter assembly
3484002	Housing assembly
3484002-99	Base
3484002-98	Cover, top
3484002-97	Cover, side
3484002-96	Cover, removable
3484002-95	Angle, external
3484002-94	Angle, internal bottom
3484002-93	Angle, internal top (left-hand)
3484002-92	Angle, internal top (right-hand)
3484002-91	Angle, internal top
3484002-90	Channel
3484002-89	Plate, front
3484002-88	Plate, mounting
3484002-87	Bracket, mirror support
3484002-86	Sleeve, mirror adjusting
3484002-85	Angle
3484003	Housing, gimbal
3484005-1 and -2	Shaft, gimbal
3484004	Gear assembly
3484017	Bracket, gear support
3484037	Shaft, gear
3484061	Spacer, gear resolver
3484062	Spacer, gear tachometer
3484027-1, -2, -3	Gear, tachometer drive
3484026	Gear, resolver
3484025-1, -2	Gear, shaft drive
3484007	Ring, primary mirror
3484008	Support, folding mirror (small)
3484009	Ring, clamp
3484010	Support, mirror
3484011	Bracket, support
3484012	Mount, mirror
3484013	Ring, housing attachment
3484014	Housing, base compartment
3484015	Angle, attach
3484016	Spool, wire assembly
3484018	Shaft, gear
3484019	Spring, preload
3484020	Ring, housing pointing
3484021	Housing, pointing mirror
3484022	Clamp, pointing mirror
3484023	Ring, secondary mirror
3484024	Gear, drive
3484028	Clamp, ring
3484029	Plate, mirror mounting
3484030	Plate, IMC stop
3484031	Bracket, switch mounting
3484034	Shim, preload (half)
3482066	Mirror, pointing
3482067	Mirror, large folding
3482068	Mirror, primary
3482068-98	Mirror
3482068-99	Mount
3482069	Mirror, secondary
3482070	Mirror, small folding
3482071	Mirror, IMC
3482072	Mirror, relay
3482151	Aluminum mirror notes
3482106	Mirror, pre-expander primary
3482107	Mirror, pre-expander secondary
3482108	Mirror, pre-expander large folding
3482109	5.77x pre-expander O&M subassembly
3482110	Beryllium mirror notes
3484063	Ring inner
3484064	Cover, gear
3484065	Block, zero positioner lock
3484066	Support, positioner pin
3484067	Plate, IMC stop

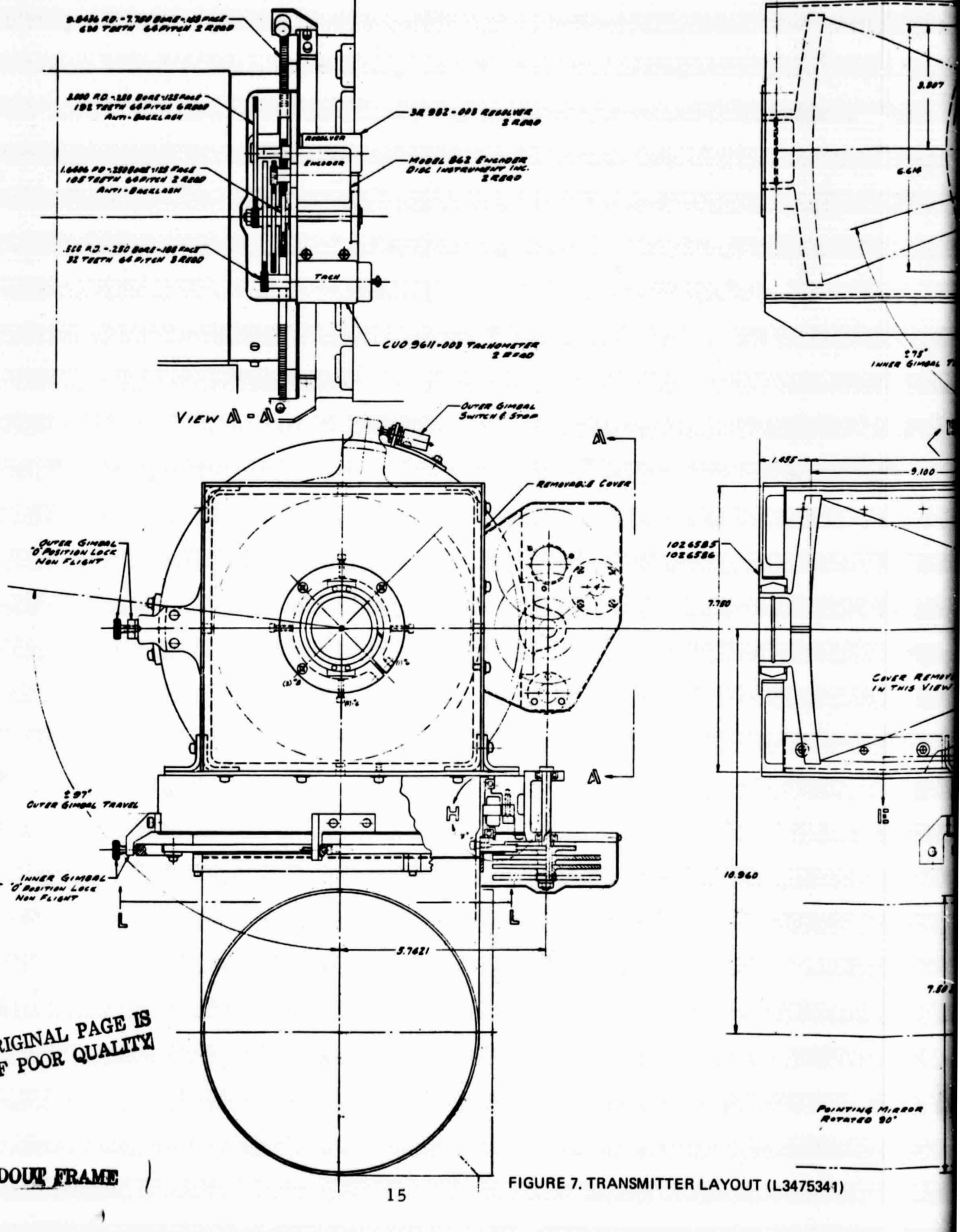

FOLDOUT FRAME

FIGURE 7. TRANSMITTER LAYOUT (L3475341)

80322-7

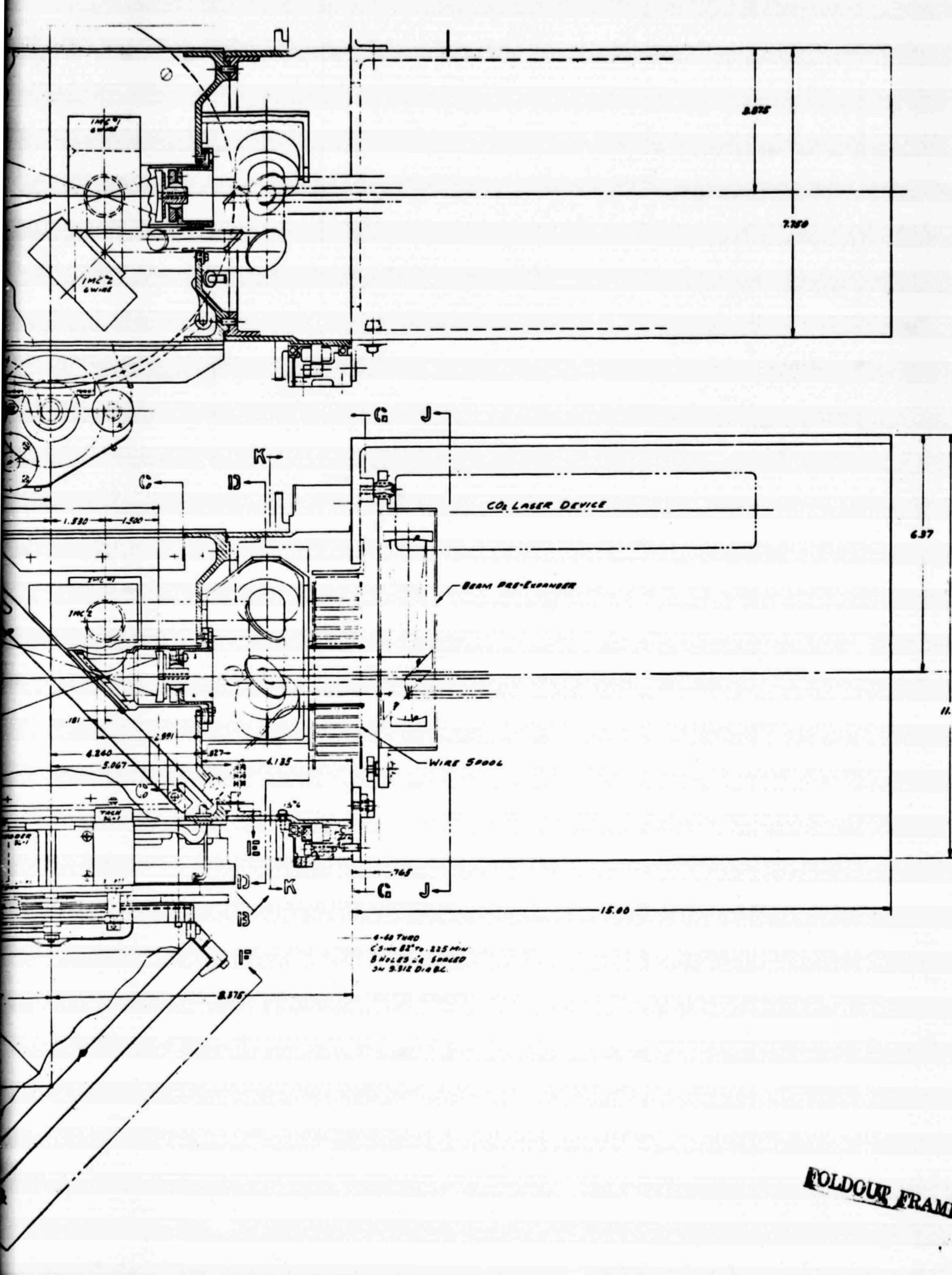

FOLDOUT FRAME 2

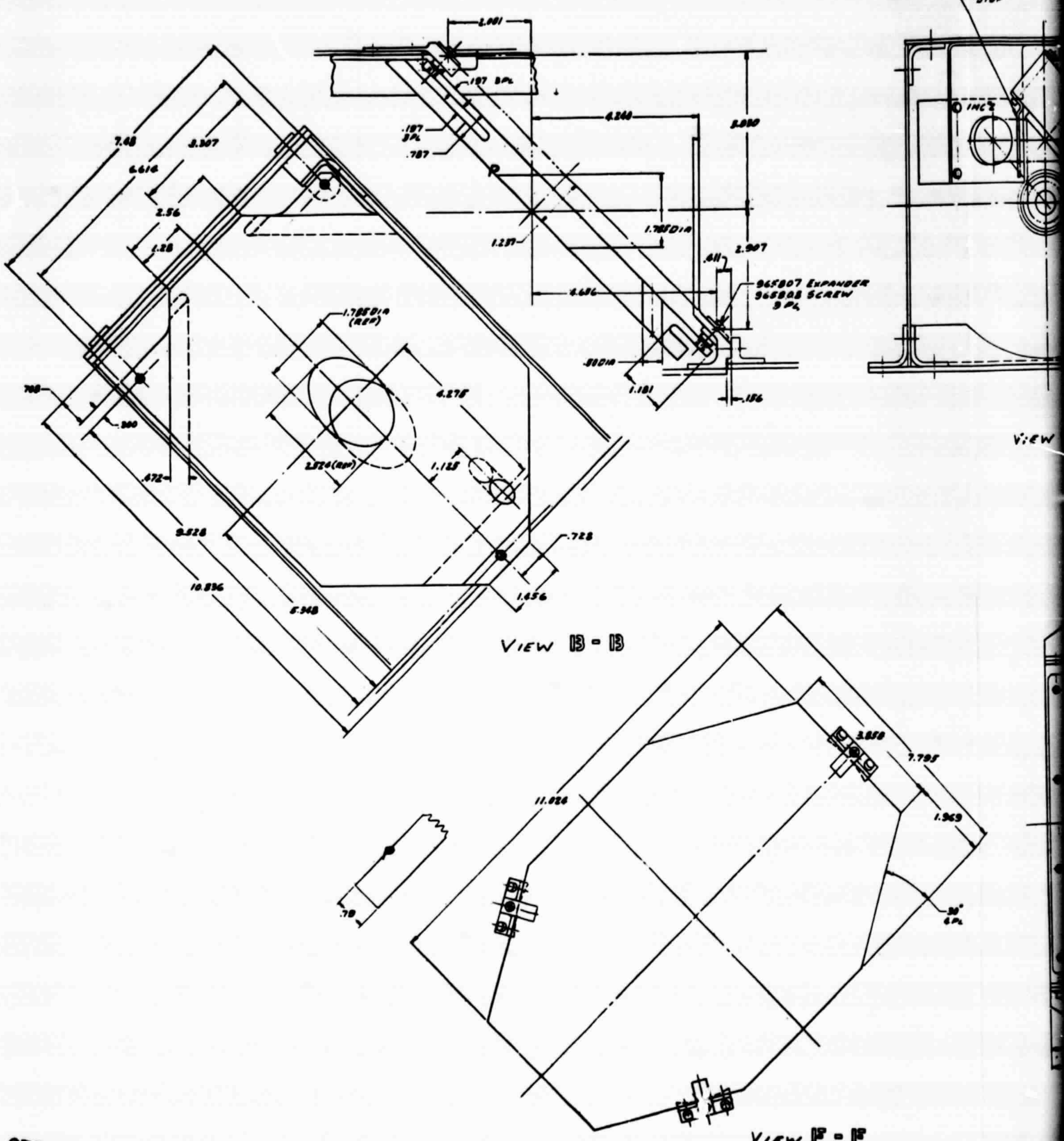

FIGURE 7 (CONTINUED). TRANSMITTER LAYOUT

50322-8

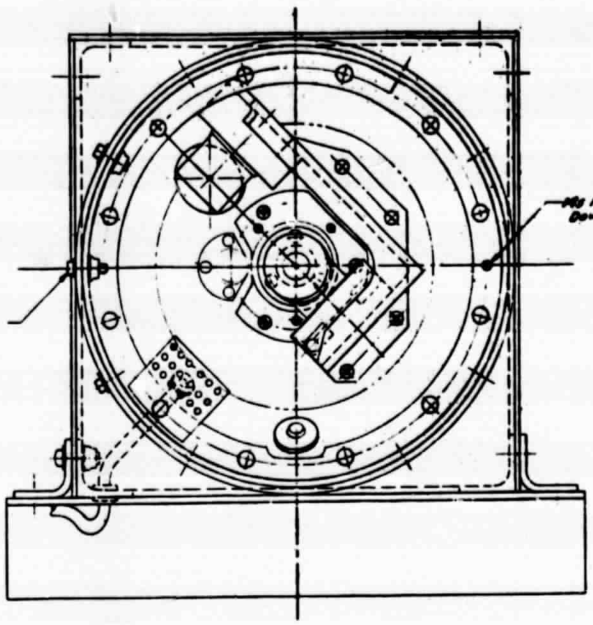

VIEW D-D

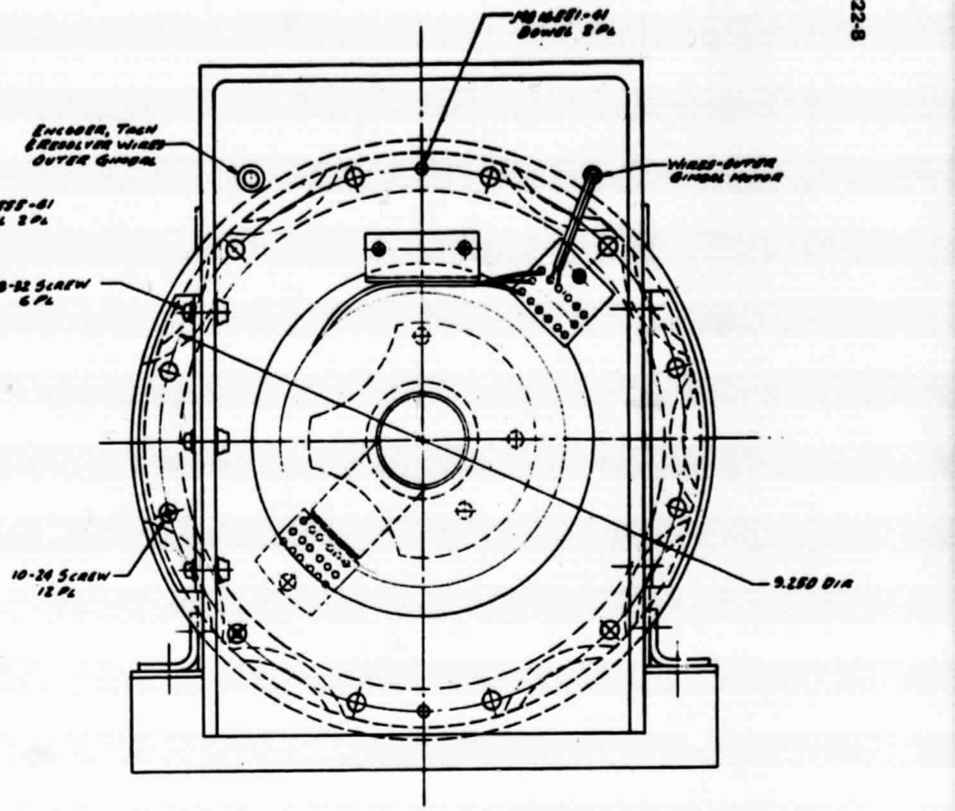

VIEW G-G

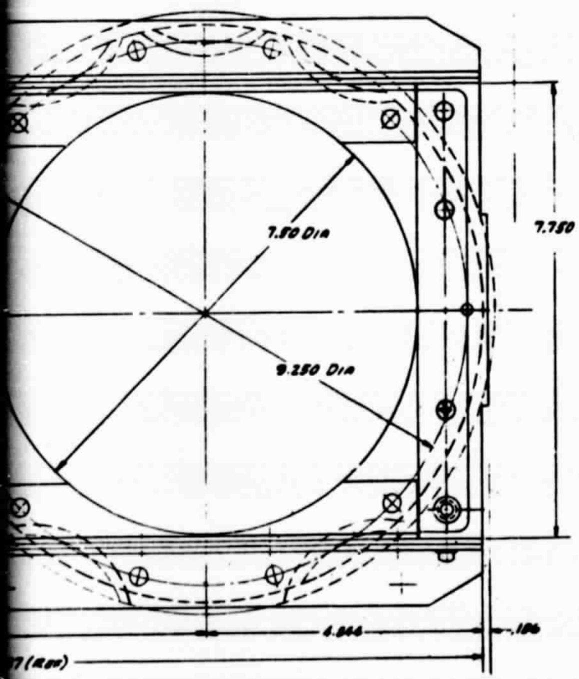

VIEW E-E

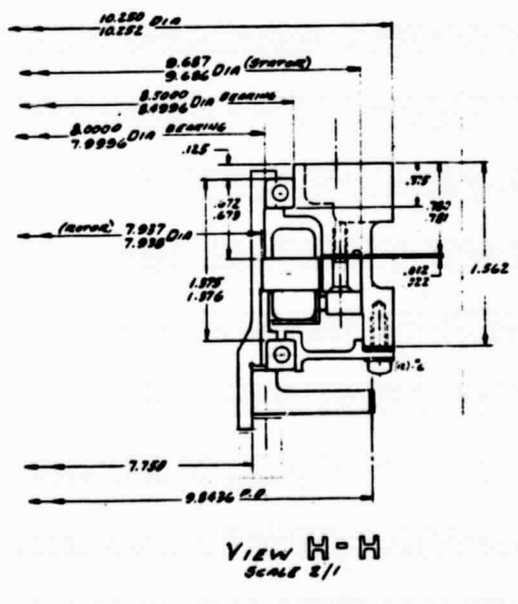

VIEW H-H
SCALE 2/1

FOLDOUT FRAME 2

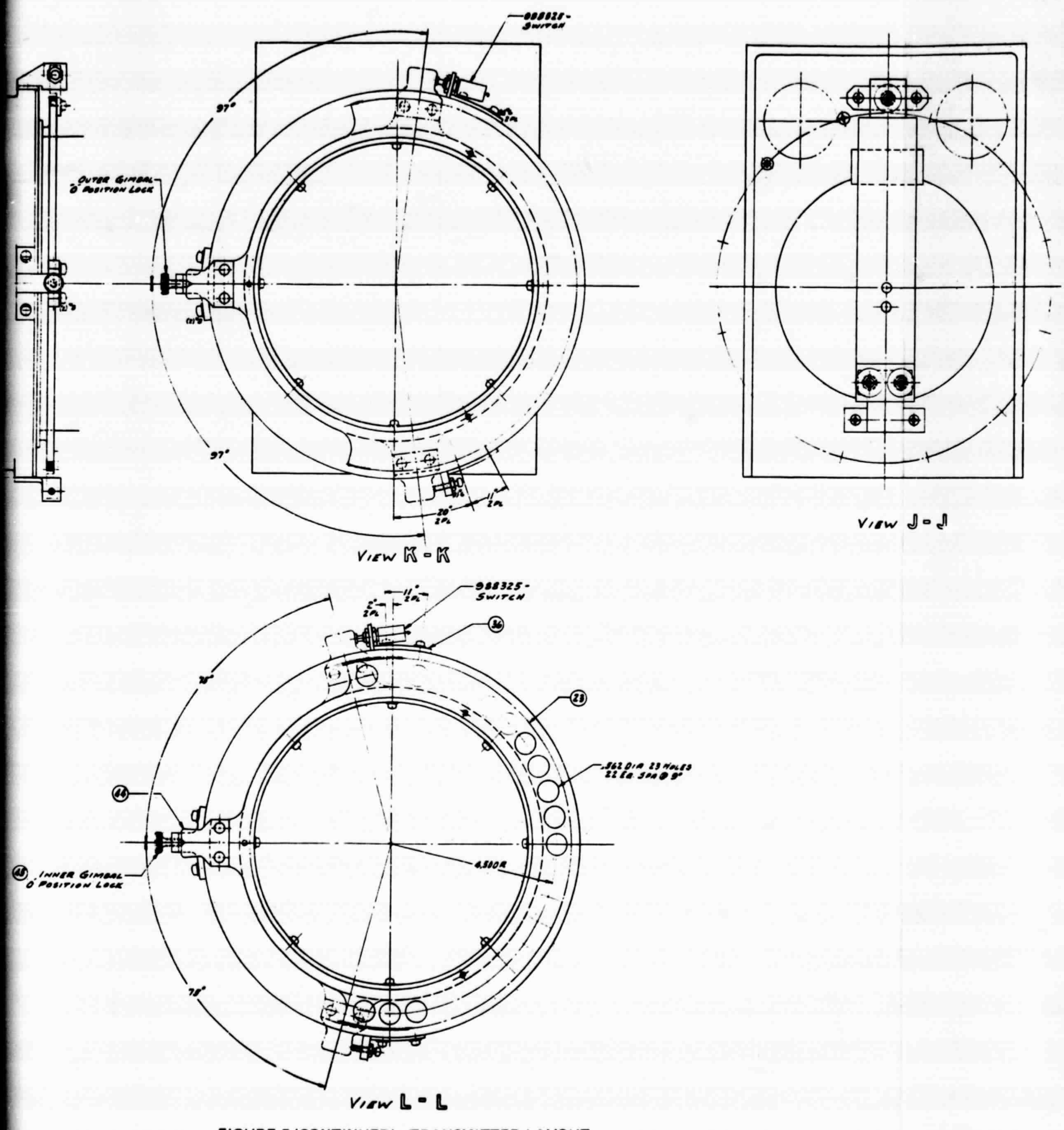

FIGURE 7 (CONTINUED). TRANSMITTER LAYOUT

50322-9

6. ANALYSIS TASKS

In addition to hardware, the scope of this program (originally an analysis program) includes two complete link analysis volumes. Much of the work for these volumes was conducted in the early months of the program and is presently scattered throughout a large number of reports, notebooks, and other documents. Jim Sullivan, who performed much of the analysis, has been assigned to collect and assemble information for these reports. Although the report outlines contained in the statement of work for this contract are presently obsolete, Mr. Sullivan will work to these outlines and will indicate where outline topics are not applicable or where information has not been generated.

A rough draft of these reports is being assembled during the next quarter for submittal to the customer. Several sections of the reports are highly dependent on customer input, especially true of sections dealing with ground stations. It is hoped that this information will be available from the customer to be added to these reports.

7. OPTOMECHANICAL SUBSYSTEM OF 10 μm RECEIVER MEASUREMENTS

The measurement program will integrate the waveguide local oscillator, servo drive electronics, and AIL receiver with its doppler tracking electronics into the optomechanical subsystem (OMSS). This will provide a complete optical heterodyne receiver that will be tested and evaluated to determine its performance characteristics. The components to be integrated were developed under contracts NAS 5-21859, NAS 5-23119, NAS 5-23183, and NAS 5-23211.

During this reporting period, receiver integration was completed and the receiver operated against a 10.6 μm source. Acquisition and tracking were demonstrated and the receiver was successfully operated over a 7 mile range. Quantitative measurements will be conducted when suitable test gear becomes available during the next quarter.

Problems encountered with the receiver front end as described in the last report have all been resolved. The electronic failures were repaired; the preamplifier was replaced with a NASA furnished unit; and the photodiode was replaced with the spare unit.

Using a 10.6 μm laser in conjunction with a dual wavelength collimator, acquisition and tracking were demonstrated. Qualitative performance appears to duplicate the results achieved during servo testing using a non-coherent 6328Å source. Two difficulties were encountered with laboratory tests. First, the lasers available for testing the system have degraded performance and are very difficult to force into single mode operation. The result is a very unstable signal for tracking. Secondly, the sensitivity of the heterodyne detection process is so high that extraneous scattered energy

within the laboratory affects operation, and the receiver will occasionally lock onto a scattered sidelobe or bright spot within its field of view. Despite these difficulties, performance has been very good.

Quantitative measurements of NEP, BER, and tracking parameters will require additional test gear now under development or on order. BER measurements will require a modulated laser source and driver now being developed under separate contract. NEP measurements will require a calibrated black body source which has been ordered. Tracking parameters will require a better laboratory laser and reduction of the sidelobes and scattered energy from the collimator. Steps are being taken to accomplish these tasks.

Figure 8 is a photograph of the completed receiver optical head. The local oscillator, Stark cell, and associated optics are visible. The gimbal and large pointing mirror were removed for this picture to show the relationship between laser and combining optics mounted on the optical bridge. The complete receiver system is shown in Figure 9. The optical head is

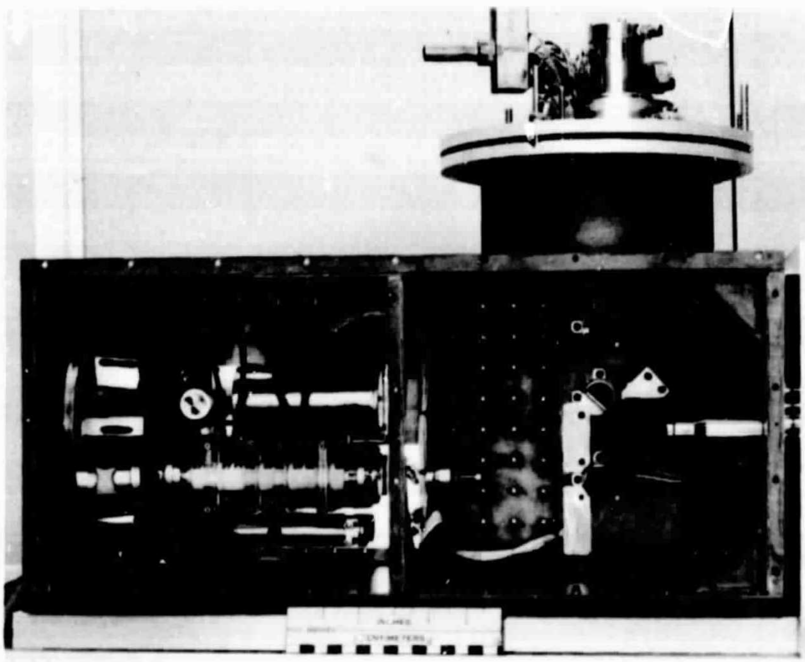

FIGURE 8. 10.6 MICROMETER RECEIVER OPTICAL HEAD (PHOTO 75-37363)

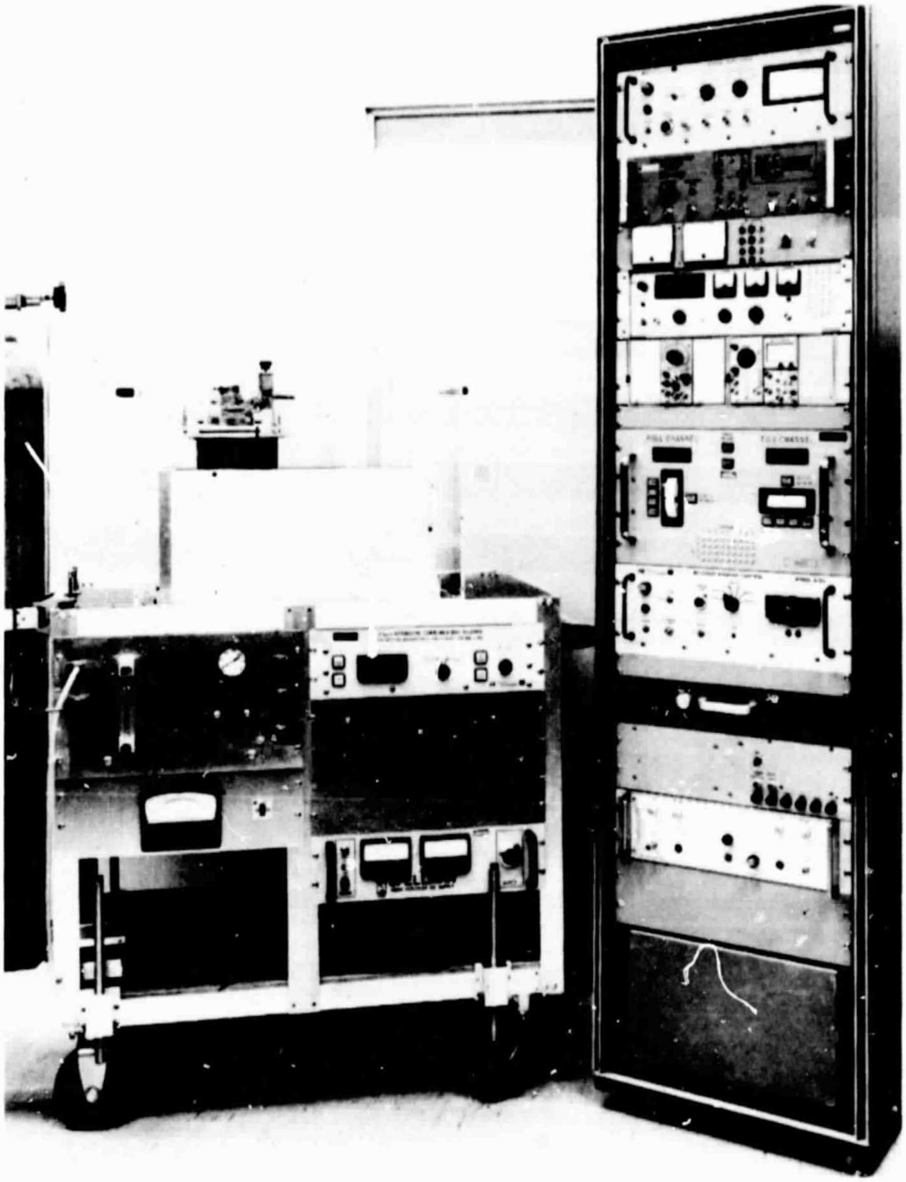

FIGURE 9. FULLY INTEGRATED RECEIVER SYSTEM (PHOTO 75-37362)

mounted on the aluminum structure on top of the cart. The aluminum support acts as a rigid test mount and also as a large heat sink to dissipate the local oscillator heat. Also on the cart are the cryostat controls, laser power supply, start/ballast circuit, and the receiver front end control. The cart can be raised off its wheels to allow operation of the receiver without removing the optical head.

The console contains the rest of the electronics. From the top, there is the laser signal simulator, BER test set, and receiver interface and monitoring panel. The fourth panel is the local oscillator Stark cell control and laser monitoring electronics. The fifth panel is a series of test instruments, including a function generator, sweep generator, and x-y monitor.

The x-y monitor is used to display the position of the two IMCs. A digital voltmeter with temperature measuring capability was added to this panel after the photograph was taken.

The large panel below the test instruments is the servo control and monitor. Two edge mounted meters and two 5 digit counters display the position of the large pointing gimbal with a readout resolution of 0.002° (35 μrad). The AIL receiver control panel is next, followed by a combination storage drawer and writing desk. The servo system power supply panel, high voltage IMC driver amplifier, and the AIL receiver complete the console.

Range Tests

During the past 2 months the receiver system was located in a rented room 7 miles south of the Hughes El Segundo facility. A link was established between these two locations for demonstration and testing of another optical system. For these tests, the AIL receiver subsystem was bypassed and a 30 MHz FM receiver was substituted, since the transmitter source was FM modulated. Figure 10 is a block diagram of the modified receiver.

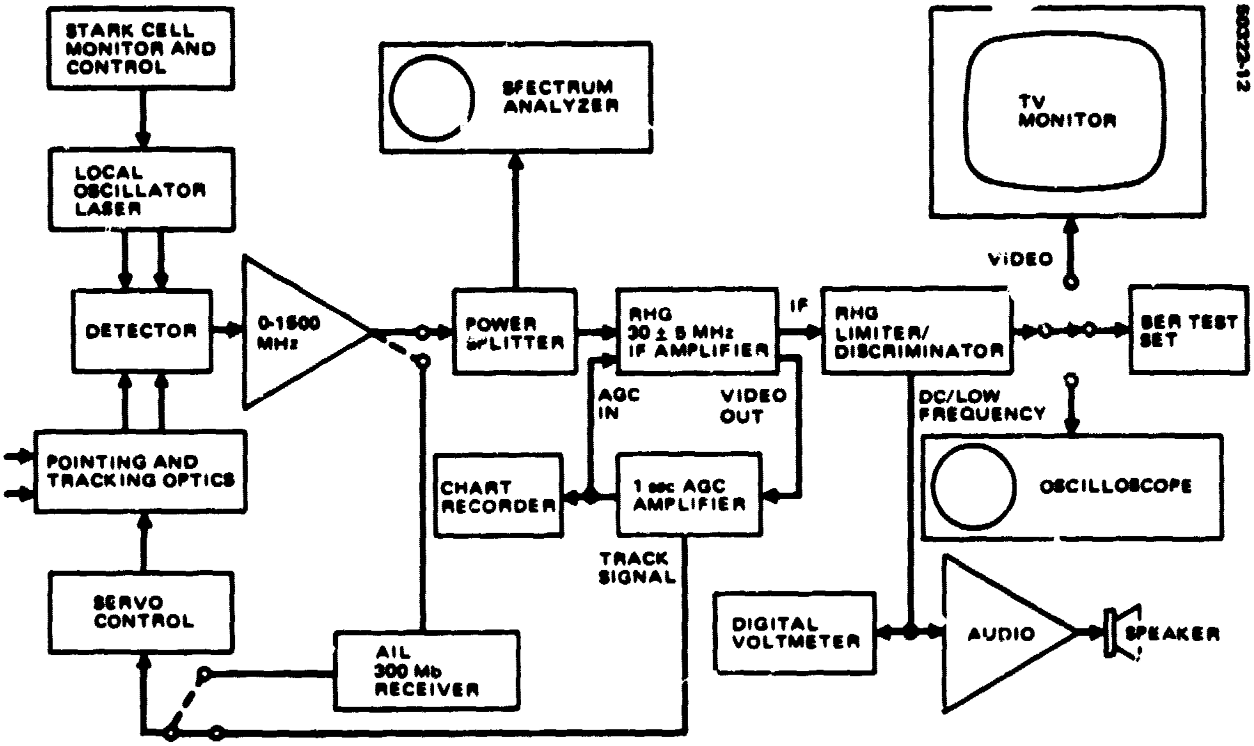

FIGURE 10. 10.6 MICROMETER RECEIVER MODIFICATION FOR 7 MILE LINK TESTS

Figure 11 is a sample of an AGC recording taken during these tests. The top two traces, identical except for time scale, are typical of the scintillation level at this site. The 30 dB peak-to-peak fluctuations are severe, best explained by an examination of the receiver site. The receiver was located on an eighth floor concrete balcony and was aimed within 11° parallel to the building side. A swimming pool, concrete deck, and plowed field were located in close proximity below the balcony. A 15 to 20 mph wind completed a typical day. The turbulence in the near field of the receiver caused by this combination of conditions was severe. In addition, there were power lines and a power line support tower in the transmitter illumination field of view, leading to a strong possibility of multipath interference. The end result was instability in the servo tracking loop. The system would track for short periods of time, then jump to a new angular location, and continue tracking. This would occur every few seconds as different sidelobes would exceed the level of previous signals. Thus, for most testing the tracking loop was disabled and the system pointed by open loop.

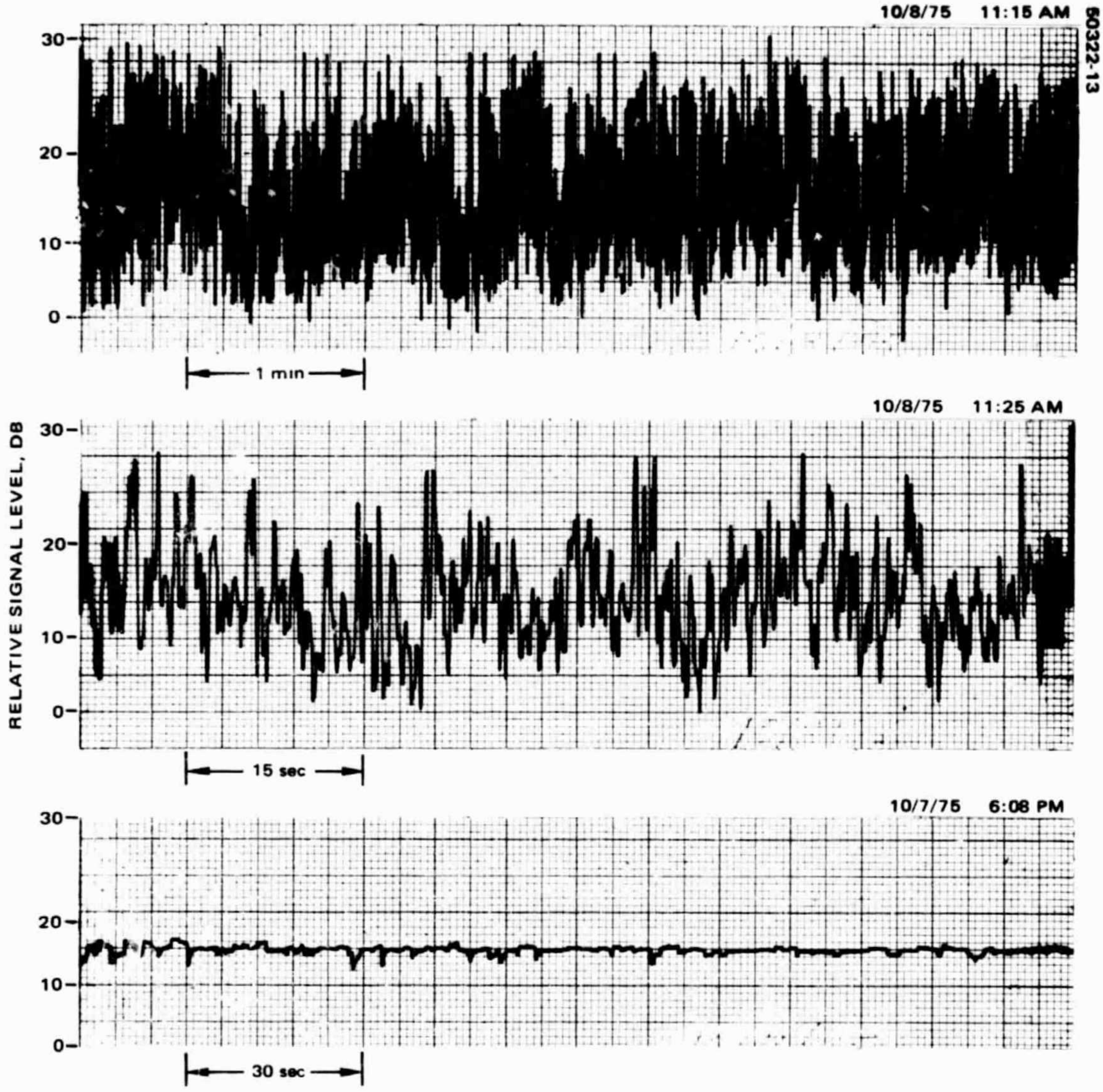

FIGURE 11. AGC LEVEL FOR TYPICAL DAY AND QUIET EVENING

During one evening run (about sunset), the scintillation level dropped dramatically to about 3 dB peak-to-peak. A sample of the AGC signal for this run is shown in the lower trace of Figure 11. During this period, the servo system would acquire and track reliably, thereby confirming suspicion that severe scintillation caused tracking problems. Figure 12 is a sample

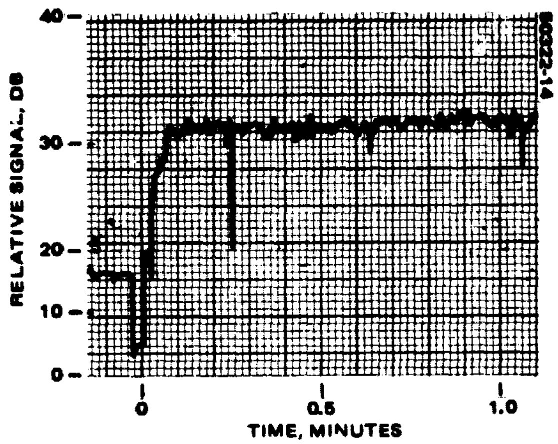

FIGURE 12. AGC LEVEL DURING ACQUISTION AND TRACKING

of the AGC signal during acquisition. The reduced signal level immediately after acquisition is caused by the large angle conical scan; there is about a 2 dB increase when the scan angle is reduced.

During the next quarter the receiver will return to the laboratory for definitive measurements; the antenna pattern will be measured to determine the sidelobe level and distribution; and NEP will be measured. Depending on availability of test equipment, some of the servo tests will be repeated to confirm performance at 10.6 μm relative to measured performance at 0.6328 μm.